HHS Public Access

Author manuscript

Int J Radiat Oncol Biol Phys. Author manuscript; available in PMC 2016 February 01.

Published in final edited form as:

Int J Radiat Oncol Biol Phys. 2015 February 1; 91(2): 393–400. doi:10.1016/j.ijrobp.2014.10.041.

Nanoparticles based brachytherapy spacers for delivery of localized combined chemo-radiation therapy

Rajiv Kumar, Ph.D.[1,3], **Jodi Belz, B.S.**[1], **Stacey Markovic, M.S.**[2], **Tej Jadhav, M.S.**[1], **William Fowle, M.S.**[1], **Mark Niedre, Ph.D.**[2], **Robert Cormack, Ph.D.**[3], **Mike G Makrigiorgos, Ph.D.**[3], and **Srinivas Sridhar, Ph.D.**[1,3]

[1]Nanomedicine Science and Technology Center, Northeastern University, Boston, MA 02115

[2]Department of Electrical and Computer Engineering, Northeastern University, Boston, MA USA

[3]Department of Radiation Oncology, Brigham and Women's Hospital, Dana-Farber Cancer Institute and Harvard Medical School, Boston, MA USA

Abstract

Purpose—In radiation therapy (RT), brachytherapy inert source spacers are commonly used in clinical practice to achieve high spatial accuracy. These implanted devices are critical technical components of precise radiation delivery but provide no direct therapeutic benefits.

Materials and Methods—Here we have fabricated Implantable Nanoplatforms or Chemo-Radiation Therapy (INCeRT) spacers loaded with silica nanoparticles (SNPs) conjugated containing a drug, to act as a slow release drug depot for simultaneous localized chemo-radiation therapy. The spacers are made of poly(lactic-coglycolic) acid (PLGA) as matrix, were physically identical (size) to the commercially available brachytherapy spacers (5mm×0.8mm). The silica nanoparticles with diameter 250nm conjugated with near infrared fluorophore Cy7.5 as a model drug and the INCeRT spacers were characterized in terms of size, morphology and composition using different instrumentation techniques. The spacers were further doped with anticancer drug, docetaxel. We have evaluated the in vivo stability, biocompatibility and biodegradation of these spacers in live mouse tissues.

Results—The electron microscopy studies showed that nanoparticles were distributed throughout the spacers. These INCeRT spacers remained stable and can be tracked using optical fluorescence. In vivo optical imaging studies showed a slow diffusion of nanoparticles from the spacer to the adjacent tissue as opposed to the control Cy7.5-PLGA spacer which showed rapid disintegration in a few days with a burst release of Cy7.5. The docetaxel spacers showed suppression of tumor growth as opposed to control mice over 16 days.

Corresponding Author's Name and Mailing Information: Rajiv Kumar and Srinivas Sridhar, Ph.D., Nanomedicine Science and Technology Center, 110 Forsyth St 111 Dana, Northeastern University, Boston MA 02115, Phone: (617) 373-2948, Fax: 617-373-2823. r.kumar@neu.edu (R Kumar) and s.sridhar@neu.edu (S Sridhar).

Conflict of Interest: None

Conclusions—The imaging with the Cy7.5-spacer and therapeutic efficacy with docetaxel-spacers supports the hypothesis that INCeRT spacers can be used for delivering the drugs in slow, sustained manner in conjunction with brachytherapy, as opposed to rapid clearance of the drugs when administered systemically. The results demonstrate that these spacers with tailored release profiles have potential in improving the combined therapeutic efficacy of chemo-radiation therapy (CRT).

Introduction

With an estimated 233,000 new cases of prostate cancer anticipated in 2014 in the US alone, prostate cancer is the most frequently diagnosed cancer and second leading cause of cancer death in men. (1) The treatment choices are primarily based on the prostate specific antigen (PSA) levels, biopsy grade (Gleason score), and clinical stage of a patient. (2) Radiation therapy (RT) involving brachytherapy may be used as monotherapy for early stage disease or in conjuction with other therapies for more advanced disease.(3–5) Data from two randomized trials suggests that increased radiation dose is associated with improved cancer control, but radiation dose-escalation is generally limited by the toxicity from the rectal wall and urethra receiving dose levels beyond tolerance. Following initial radiation for localized prostate cancer (PCa), between 20–30% of men may experience PSA failure. (6–7) For those with a local-only recurrence, salvage brachytherapy offers a second chance for cure, but leads to a high rate of rectal toxicity including up to 13% rate of prostate-rectum fistulas requiring colostomy in one prospective phase II study. (8–9) Inert biocompatible spacers (brachytherapy), which are frequently implanted for controlling the spatial distribution and accuracy of radiation to the prostate, are critical technical components for radiation delivery but have ‘*zero*’ direct therapeutic benefits. (10–13)

A number of chemotherapy agents are also radiosensitizers. (14–15) The chemotherapy schedules generally involve weekly intravenous delivery with elimination time scales on the order of 24 hours implying less than half the radiation fractions in a week are delivered with agent circulating. Chemotherapy dose is limited by systemic toxicities that usually prevent the use of chemotherapy through the entire course of radiation. A means of delivering focal distributions of chemotherapy agent to the prostate without systemic delivery could offer a means of increasing the synergistic effect of radiation and chemotherapy agent and improving the therapeutic ratio.

It has been proposed that the fiducials and brachytherapy spacers offer the opportunity for in-situ delivery of drugs as part of currently routine minimally invasive radiation therapy procedures.(11) Modeling of the drug distributions that could be achieved by transforming the inert fiducials or spacers into drug reservoirs, capable of sustained drug release over periods appropriate to radiation therapy, indicate that significant portions of the prostate could be radiosensitized while maintaining a localized drug distribution. Thus, there exists an opportunity to fabricate drug loaded spacers in such a way that it improves the therapeutic ratio of the brachytherapy procedure by delivering radiosensitizer to the prostate without systemic toxicity. We previously conducted a theoretical evaluation of prostate brachytherapy spacers containing slow-release polymers that elute the radio-sensitizer docetaxel. (11) The use of nanoparticles facilitates local delivery of therapeutics in high

dose to the tumor, slow and sustained release of the drugs, incorporation of imaging agents, minimal systemic drug toxicities to non-targeted organs and greater spatial distribution of the drug in the tumor. (16–19)

In this manuscript we report a novel fabrication approach for the INCeRT spacers in which the biocompatible matrix composed of PLGA polymer forms the backbone of the spacers which contains embedded silica nanoparticles in the matrix as drug/ fluorophore depot. These spacers are identical to the routinely used brachytherapy spacers in shape and size but with an additional therapeutic and diagnostic value. We have extensively explored the use of SNPs loaded with NIR fluorophore Cy7.5, as a model drug that can be visualized *in vivo*. We have also fabricated the docetaxel loaded spacers to evaluate the therapeutic response of these INCeRT spacers. The spacers were characterized by optical fluorescence studies, scanning electron microscopy (SEM), transmission electron microscopy (TEM), and Energy Dispersive Spectroscopy (EDS). The preliminary in vivo data obtained with these implanted INCeRT spacers shows great potential in developing novel therapeutic strategies, leading to localized drug delivery to tumor. This would result in preferential radiosensitization of the prostate compared to the normal structures, which can be used in combination with RT to maximize therapeutic effect.

Materials and Methods

Spacers were designed to be compatible with a preloaded needle brachytherapy technique. Diameter was chosen to fit within an 18G brachytherapy needle. Composition and length were chosen so the spacer would be rigid during insertion to ensure the appropriate spacing of brachytherapy sources, and the spacer will degrade over time once implanted into the tissue, releasing the drug locally. Details of materials used and methods for SNPs and spacers synthesis, physico-chemical characterization of nanoparticles as well as INCeRT spacers, imaging setup and analysis, and *in vivo* studies is included in the supplementary information.

Methods: Fabrication of INCeRT spacers

The synthesis of Cy7.5-SNPs was carried out using oil-in-water microemulsion method, following a previously reported protocol with several modifications. (20–21) The fabrication of spacers was carried out in two steps which involve (a) extraction of SNPs from the aqueous media and (b) by polymer extrusion along with nanoparticles. (See Supplementary Information)

Results

Figure 1a shows the schematic presentation of the structure of INCeRT spacers fabricated with PLGA matrix impregnated with SNPs. These spacers were fabricated with a range of different molecular weight of PLGA polymer with a combination of non-polar solvent systems. The slurry made with PLGA and SNPs were extruded in a controlled manner in silicon tubing which has an internal diameter similar to the diameter of the commercial brachytherapy spacers. These nanoparticles doped INCeRT spacers were cut into lengths similar to commercial spacers (5 mm).

Figure 1b shows the images of the fabricated INCeRT spacers (left and middle panel) compared with the commercially available spacers (right panel). All these spacers were identical in terms of morphology, dimensions and structural integrity. The 'dual' release mechanism involves the dissolution of PLGA in biological fluid to release the nanoparticles in extracellular space, after which in a second phase these nanoparticles, upon interaction with cellular fluids, will start releasing the encapsulated drug in a sustained manner at the target site. (22) The SNPs platform provides a method for delivery of drugs/imaging agents, with ease of surface modification, covalent conjugation to fluorophores and size modulation. (20) The rationale behind using PLGA as a matrix polymer lies in its biocompatibility, biodegradability and low glass transition temperature, which have been studied previously as a host matrix for different chemotherapeutics in implants. (23–24) The fluorescence from the conjugated Cy7.5, helped tracking the nanoparticles which otherwise was very difficult with drug loaded nanoparticles. (25–26)

The release profile of the Cy7.5 from Cy7.5-spacers in buffer showed gradual increase in fluorescence intensity till day 4 as opposed to Cy7.5-Silica spacer in which the fluorescence intensity kept increasing over 7 days. Also, the absence of fluorescence in the flow through indicated covalent conjugation of Cy7.5 to SNPs and thus tracking of intact nanoparticles. (figure S1) Figure 2 shows the time space profile of the different formulations (free dye, 30nm Cy7.5-SNPs and 200nm Cy7.5-SNPs) in agar phantoms based on diffusion through the agar matrix over time. The result showed a rapid diffusion of free dye within 1hr whereas 30 and 200 nm SNPs showed size dependent diffusion through the matrix over 15 days.

The characterization data of the Cy7.5-SNPs showed a typical fluorescence emission peak at λ_{max} 820 nm with a slight bathochromic shift for conjugated nanoparticles (figure S2a) which can be attributed to slight aggregation of the dye molecules in core of Cy7.5-SNPs. (27) The TEM image of SNPs showed a spherical morphology with a size of 254±5 nm (average of ~100 nanoparticles) with unimodal distribution (figure S2b). The DLS data also confirmed the size to be 260±8 nm (data not shown). This slight increase in size can be attributed to the hydrodynamic diameter of the SNPs. (28) For both the formulations (encapsulated or conjugated Cy7.5), as expected the surface charge remained the same, i.e. −25 mV. The pore size for the silica nanoparticles in 250 nm size was previously reported to be approximately 2.3 nm.(29) The size of ~250 nm was selected to increase the percentage loading of the drug per nanoparticle, however we have also tested smaller size nanoparticles (30 nm) which have higher capability to penetrate the tumor matrix.

After incorporation of the SNPs into the PLGA matrix, the INCeRT spacers were analyzed by SEM for surface morphology analysis and the distribution pattern of the SNPs into PLGA matrix. Figure 3a and 3b shows the SEM image of lateral and transverse surface of the fabricated Cy7.5-SNPs-spacers. The SEM image showed a solid structure without any air spaces/vacuoles with a smooth outer surface. At higher magnification, it can be visualized from the lateral view that the SNPs were embedded in the PLGA matrix in patches all along the spacer length (Figure 3c). The transverse section showed that nanoparticles accumulated more towards the core of the spacer. To qualitatively differentiate between the electron dense SNPs (relative to PLGA polymer) from PLGA, we have used

back scattered electron (BSE) imaging technique (figure 3d). The increase in contrast between the silica patches in the dark PLGA background confirms presence of SNPs. To confirm it further we have carried out EDS analysis by selecting various ROI on the spacers (bright patches) and the results showed presence of silicon (Si) in the ROI along with carbon and oxygen (figure 3f).

Further, to see the distribution pattern and visualize the nanoparticles inside PLGA matrix, we have used freeze fracture technique by flash freezing the spacers in liquid N_2 and fracturing them. Figure 3e clearly shows that the fractured surface has well defined spherical grooves. We believe that these groves are the impressions of SNPs which were shredded/ fallen off while fracturing the spacers. The size of the individual grooves was on an average 260 nm, which very well correlates with the TEM size of the SNPs indicating minimal aggregation of SNPs. Further, to confirm our technique for visualizing nanoparticles in PLGA matrix by this method, we have doped electron dense gold nanoparticles in the PLGA matrix. The results clearly indicated that although the nanoparticles were present in patches in PLGA matrix, the aggregation between nanoparticles were minimal. (figure S3)

Live animal fluorescence imaging studies were carried out with mice implanted with INCeRT spacers with approved IACUC protocols (figure 4). The fluorescence intensity of the control spacer (Cy7.5-spacer; upper right) kept decreasing and completely disappeared by day 14. This can be attributed to the rapid release of Cy7.5 incorporated in PLGA matrix over time, which resulted in a decrease of local Cy7.5 concentration in the spacer. The released Cy7.5 from the spacer, which was distributed around the spacer, was difficult to measure because the intact skin provided a barrier for the excitation light to penetrate and excite such low concentrations of Cy7.5. The quantification of the fluorescence intensity at half width maximum for the lower left Cy7.5-SNPs-spacer showed a constant increase for nanoparticles doped spacer within the same time duration of 14 days. (figure 4b) From the figure it can be clearly visualized that Cy7.5 fluorescence is very stable and localized around the spacer suggesting a slow diffusion of SNPs from the PLGA matrix. Also, it is worth noting that for the spacers with Cy7.5-SNPs, we are tracking the nanoparticles rather than free dye as the dye molecules are covalently conjugated into the silica core.

The spacers implanted in the upper left flank of the mice showed a very similar result as observed for the lower left spacer. Despite the minimal diffusion, stable fluorescence intensity suggests that the release of the nanoparticles from the spacers as well as the degradation of the PLGA was not very rapid and the silica doped spacers maintained structural integrity in both the intradermal and intratumoral environment. The quantitation of the intensity from the figure indicated a constant increase in intensity for Cy7.5-SNPs-spacers for 14 days as opposed to Cy7.5-spacer which kept decreasing over the same time frame. We have further carried out preliminary size dependent diffusion of nanoparticles (30 and 200 nm SNPs in spacers) which also confirmed minimal diffusion for bigger size nanoparticles. (Figure S4)

Figure 5 shows the fluorescence images of the dissected animal by removing the skin and exposing the implanted spacers. The lower left spacer (Cy7.5-SNPs-spacers) showed localized fluorescence which can be attributed again to the intact spacer however for the

upper right flank spacer (Cy7.5-spacer) the fluorescence emission can be observed from a wide area around the spacer. Also, it was interesting to observe that while the left flank spacer maintained its integrity, the upper right flank spacer looked like a white thread and altogether dissociated into small pieces. Also, it was very encouraging to observe the fluorescence emission from the muscles where the lower left spacer was implanted. Since the spacer was still attached to the skin (figure 5c) and the area exactly under that showed the emission, it clearly indicates that small populations of nanoparticles have been released from the spacer. Also, since Cy7.5 was conjugated to nanoparticles, the fluorescence emission has to be from the released nanoparticles. The fluorescence images of tumor showed a bright fluorescence from the location where the spacer was implanted and when we dissected the tumor laterally (lower panel) along the axis from where the fluorescence was originating, we observed that fluorescence was coming from the spacers only with very low fluorescence from surrounding tissue (figure 5e).

The pilot in vivo therapeutic studies with docetaxel INCeRT spacers implanted in tumor showed suppression of tumor growth as opposed to control mice in which tumor size kept increasing. (figure S5) The free docetaxel group also showed tumor growth suppression but associated with weight loss in all mice reflecting systemic toxicity associated with free drug. (figure S6)

Discussion

We have demonstrated the feasibility to create ‘dual’ release brachytherapy spacers that have the capacity to deliver drugs to the target without intravenous delivery. This feasibility of using different ways of incorporating chemotherapeutic/imaging agents provides an additional advantage for localized delivery of the chemotherapeutic agent by encapsulation in silica matrix and for optical tracking of drug loaded nanoparticles via covalently conjugated fluorophore like Cy7.5. (30–31)

Based on the results obtained, a detailed in vivo study with spacers fabricated with different size of nanoparticles, varying molecular weight of PLGA and further incorporation of chemotherapeutic drugs is currently underway in tumored mice model. To achieve radiosensitization of the target without simultaneously sensitizing the surrounding normal tissues requires the ability to control both the spatial and temporal distribution of the drug within the tumor. (11) Combined chemo-radiation therapy (CRT) requires synchronization of the two modalities to achieve maximum benefit. (32–33) Several drugs are being currently tested as a radiosensitizer with external beam radiation therapy (EBRT) in a large ongoing multinational randomized trial. (34) However systemic administration of these drugs have several drawbacks like high systemic toxicity, fast pharmacokinetics, limited periods of radiosensitization that are not synchronized with the radiation dosage and poor spatial distribution in tumor. (35–38) The use of nanoparticles doped spacers for localized drug delivery will provide several advantages over the conventional systemic delivery as described earlier. (39–42)

The two stage release platform presented here allows the different time constants for the release of nanoparticles from the spacer and the release of drug from the nanoparticles. The

use of nanoparticles provides a tissue residence measured in weeks making sensitization of permanent brachytherapy implants feasible. Once released from the spacer, controlling the size of the nanoparticles enables optimization of the spatial distribution. The two stage process should enable this approach to be used for a variety of radiosensitizing agents including gold nanoparticles. (43) The release profile of the nanoparticles from the spacers can be modulated by varying the molecular weight of the PLGA as well by changing the size of the nanoparticles. The presence of inert additives can further enhance the dissolution of PLGA matrix if a faster release of the nanoparticles is desired. This work is a significant advancement on earlier nanoparticle based radiosensitization (22) demonstrating the creation of a drug releasing spacer appropriate for use in needle based implantation of brachytherapy sources. We are also pursuing this approach for EBRT but with significantly different formulations which are tailored to match time scales of EBRT. It was encouraging to see the tumor suppression with the docetaxel loaded INCeRT spacers implanted in tumor with minimal observable toxicities as opposed to control mice, which lays the foundation for a large in vivo therapeutic study involving the docetaxel doped INCeRT spacers.

In summary, we report the fabrication, characterization and preliminary in vivo behavior of INCeRT spacers for applications in combined chemo-radiation therapy. These INCeRT spacers were doped with fluorescent silica 10 nanoparticles which were tracked optically in vivo in live animals to monitor the nanoparticles localization and diffusion from the spacers. Since the same nanoparticles can encapsulate anti-cancer drugs, localization of nanoparticles by optical imaging will qualitatively determine the extent of drug diffusion into the tumor. The *in vivo* imaging with the implanted spacers showed a slow degradation to release the nanoparticles from the PLGA matrix with no signs of observable or behavioral toxicological signs in animals. The preliminary in vivo therapeutic studies with docetaxel loaded INCeRT spacers showed tumor suppression. Knowing that the feasibility of NIR imaging in real time is difficult, these spacers require further in vivo studies to evaluate their application in PCa. However, these studies provide preliminary answers to some of the key parameters required to build the platform for localized drug delivery in conjunction with radiation therapy.

Supplementary Material

Refer to Web version on PubMed Central for supplementary material.

Acknowledgement

We acknowledge partial support from ARMY/W81XWH-12-1-0154, NSF DGE 0965843, HHS/5U54CA151881-02, the Electronics Materials Research Institute at Northeastern University, and Brigham and Women's Hospital.

References

1. American Cancer Society, Cancer Facts and Figures. 2014. (http://www.cancer.org/acs/groups/content/@research/documents/webcontent/acspc-042151.pdf)
2. Stangelberger A, Waldert M, Djavan B. Prostate cancer in elderly men. Rev Urol. 2008; 10:111–119. [PubMed: 18660852]
3. Nath R, Anderson LL, Meli JA, et al. Code of practice for brachytherapy physics: Report of the aapm radiation therapy committee task group no. 56. American association of physicists in medicine. Med Phys. 1997; 24:1557–1598. [PubMed: 9350711]

4. Dicker, AP.; Merrick, G.; Gomella, L., et al. Basic and Advanced Techniques in Prostate Brachytherapy. Taylor & Francis, CRC press; 2005.
5. Shipley WU, Thames HD, Sandler HM, et al. Radiation therapy for clinically localized prostate cancer: A multi-institutional pooled analysis. JAMA. 1999; 281:1598–1604. [PubMed: 10235152]
6. Zietman AL, Bae K, Slater JD, et al. Randomized trial comparing conventional-dose with high-dose conformal radiation therapy in early-stage adenocarcinoma of the prostate: Long-term results from proton radiation oncology group/american college of radiology 95-09. J Clin Oncol. 2010; 28:1106–1111. [PubMed: 20124169]
7. Kuban DA, Tucker SL, Dong L, et al. Long-term results of the m. D. Anderson randomized dose-escalation trial for prostate cancer. Int J Radiat Oncol Biol Phys. 2008; 70:67–74. [PubMed: 17765406]
8. Nguyen PL, Chen MH, D'Amico AV, et al. Magnetic resonance image-guided salvage brachytherapy after radiation in select men who initially presented with favorable-risk prostate cancer: A prospective phase 2 study. Cancer. 2007; 110:1485–1492. [PubMed: 17701957]
9. Nguyen PL, D'Amico AV, Lee AK, et al. Patient selection, cancer control, and complications after salvage local therapy for postradiation prostate-specific antigen failure: A systematic review of the literature. Cancer. 2007; 110:1417–1428. [PubMed: 17694553]
10. Lee WR. Permanent prostate brachytherapy: The significance of postimplant dosimetry. Rev Urol. 2004; 6([Suppl] 4):S49–S56. [PubMed: 16985870]
11. XXXX.
12. Friedland JL, Freeman DE, Masterson-McGary ME, et al. Stereotactic body radiotherapy: An emerging treatment approach for localized prostate cancer. Technol Cancer Res T. 2009; 8:387–392.
13. Sylvester JE, Grimm PD, Eulau SM, et al. Permanent prostate brachytherapy preplanned technique: The modern seattle method step-by-step and dosimetric outcomes. Brachytherapy. 2009; 8:197–206. [PubMed: 19433321]
14. Tishler RB, Geard CR, Hall EJ, et al. Taxol sensitizes human astrocytoma cells to radiation. Cancer research. 1992; 52:3495–3497. [PubMed: 1350755]
15. Castro Kreder N, Van Bree C, Franken NA, et al. Effects of gemcitabine on cell survival and chromosome aberrations after pulsed low dose-rate irradiation. Journal of Radiation Research. 2004; 45:111–118. [PubMed: 15133298]
16. Jong WH, Borm PJ. Drug delivery and nanoparticles: Applications and hazards. Int J Nanomedicine. 2008; 3:133–149. [PubMed: 18686775]
17. XXXX.
18. Parveen S, Misra R, Sahoo SK. Nanoparticles: a boon to drug delivery, therapeutics, diagnostics and imaging. Nanomedicine. 2012; 8:147–166. [PubMed: 21703993]
19. Brigger I, Dubernet C, Couvreur P. Nanoparticles in cancer therapy and diagnosis. Adv. Drug Delivery Rev. 2002; 54:631–651.
20. XXXX.
21. XXXX.
22. XXXX.
23. Makadia HK, Siegel SJ. Poly lactic-co-glycolic acid (plga) as biodegradable controlled drug delivery carrier. Polymers-Basel. 2011; 3:1377–1397. [PubMed: 22577513]
24. Lu JM, Wang XW, Marin-Muller C, et al. Current advances in research and clinical applications of plga-based nanotechnology. Expert Rev Mol Diagn. 2009; 9:325–341. [PubMed: 19435455]
25. Ohulchanskyy TY, Roy I, Goswami LN, et al. Organically modified silica nanoparticles with covalently incorporated photosensitizer for photodynamic therapy of cancer. Nano Lett. 2007; 7:2835–2842. [PubMed: 17718587]
26. Burns A, Ow H, Wiesner U. Fluorescent core-shell silica nanoparticles: towards 'Lab on a particle' architectures for nanobiotechnology. Chem Soc Rev. 2006; 35:1028–1042. [PubMed: 17057833]
27. Sahoo Y, Goodarzi A, Swihart MT, et al. Aqueous ferrofluid of magnetite nanoparticles: Fluorescence labeling and magnetophoretic control. J Phys Chem B. 2005; 109:3879–3885. [PubMed: 16851439]

28. De Palma R, Peeters S, Van Bael MJ, et al. Silane ligand exchange to make hydrophobic superparamagnetic nanoparticles water-dispersible. Chem Mater. 2007; 19:1821–1831.
29. Slowing II, Trewyn BG, Giri S, et al. Mesoporous silica nanoparticles for drug delivery and biosensing applications. Adv Funct Mater. 2007; 17:1225–1236.
30. Ghosh SK, Kim P, Zhang X, et al. A Novel Imaging Approach for Early Detection of Prostate Cancer Based on Endogenous Zinc Sensing. Cancer Res. 2010; 70:6119–6127. [PubMed: 20610630]
31. Boutet J, Herve L, Debourdeau M, et al. Bimodal ultrasound and fluorescence approach for prostate cancer diagnosis. J Biomed Opt. 2009; 14:064001–064007. [PubMed: 20059239]
32. Sanfilippo N, Hardee ME, Wallach J. Review of chemoradiotherapy for high-risk prostate cancer. Rev Recent Clin Trials. 2011; 6:64–68. [PubMed: 20868349]
33. Bolla M, Hannoun-Levi JM, Ferrero JM, et al. Concurrent and adjuvant docetaxel with three-dimensional conformal radiation therapy plus androgen deprivation for high-risk prostate cancer: Preliminary results of a multicentre phase ii trial. Radiother Oncol. 2010; 97:312–317. [PubMed: 20846737]
34. Study NCT00116142. Hormone Suppression and Radiation Therapy for 6 Months With/Without Docetaxel for High Risk Prostate Cancer. http://www.clinicaltrials.gov/ct2/show/study/NCT00116142
35. Patel KJ, Tredan O, Tannock IF. Distribution of the anticancer drugs doxorubicin, mitoxantrone and topotecan in tumors and normal tissues. Cancer Chemother Pharmacol. 2013; 72:127–138. [PubMed: 23680920]
36. Lin JH, Lu AY. Role of pharmacokinetics and metabolism in drug discovery and development. Pharmacol Rev. 1997; 49:403–449. [PubMed: 9443165]
37. Mittal G, Sahana DK, Bhardwaj V, et al. Estradiol loaded plga nanoparticles for oral administration: Effect of polymer molecular weight and copolymer composition on release behavior in vitro and in vivo. J Control Release. 2007; 119:77–85. [PubMed: 17349712]
38. Szakacs G, Paterson JK, Ludwig JA, et al. Targeting multidrug resistance in cancer. Nat Rev Drug Discov. 2006; 5:219–234. [PubMed: 16518375]
39. Italia JL, Bhatt DK, Bhardwaj V, et al. Plga nanoparticles for oral delivery of cyclosporine: Nephrotoxicity and pharmacokinetic studies in comparison to sandimmune neoral. J Control Release. 2007; 119:197–206. [PubMed: 17399839]
40. Papahadjopoulos D, Allen TM, Gabizon A, et al. Sterically stabilized liposomes: Improvements in pharmacokinetics and antitumor therapeutic efficacy. Proc Natl Acad Sci U S A. 1991; 88:11460–11464. [PubMed: 1763060]
41. M F. Cancer nanotechnology: Opportunities and challenges. Nat Rev Cancer. 2005; 5:11. [PubMed: 15630411]
42. Peer D, Karp JM, Hong S, et al. Nanocarriers as an emerging platform for cancer therapy. Nat Nanotechnol. 2007; 2:751–760. [PubMed: 18654426]
43. XXXX.

Summary

This work describes the creation of brachytherapy spacers for in-situ release of drug eluting nanoparticles to provide tissue residence and sustained drug release with time constants appropriate for permanent brachytherapy. The in-vivo behavior of spacers was studied by optical fluorescence imaging of mice implanted with spacers releasing free dye molecules or dye eluting nanoparticles, and demonstrated sustained release for synchronous chemoradiation therapy to enhance the therapeutic ratio of permanent prostate implants.

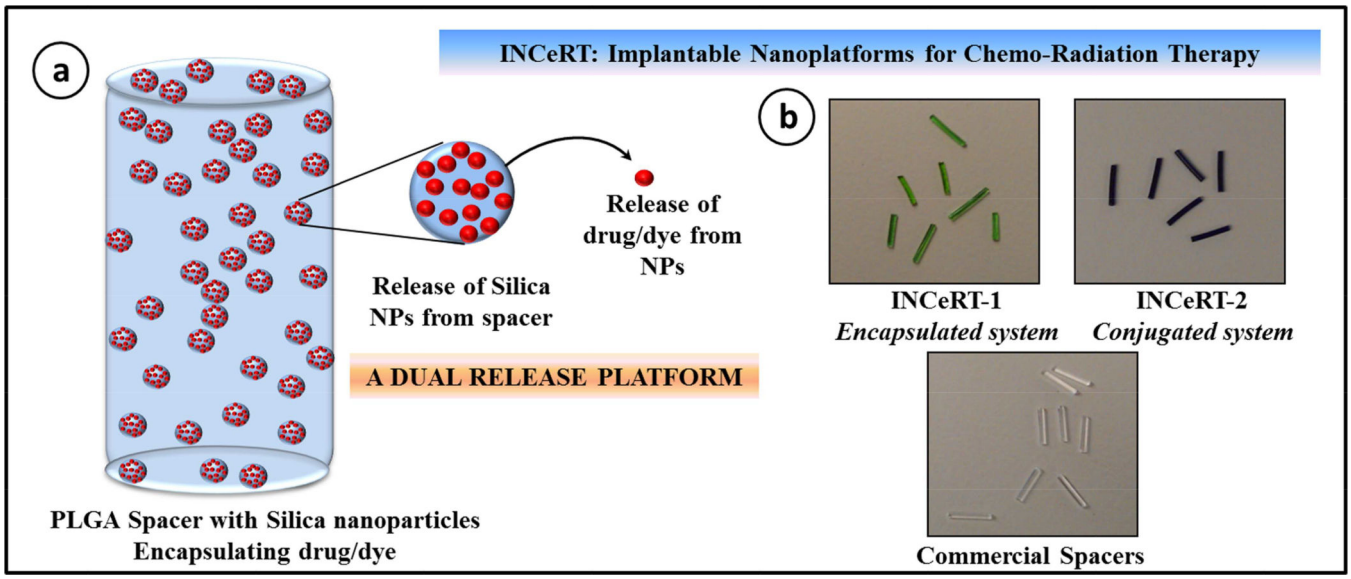

Figure 1.

(a) Schematic representation of the modified brachytherapy spacer formulated using PLGA polymer impregnated with Cy7.5 labelled SNPs. (b) The physical appearance of the as synthesized modified brachytherapy spacers with different formulations of SNPs and comparison with commercial spacers used in clinics.

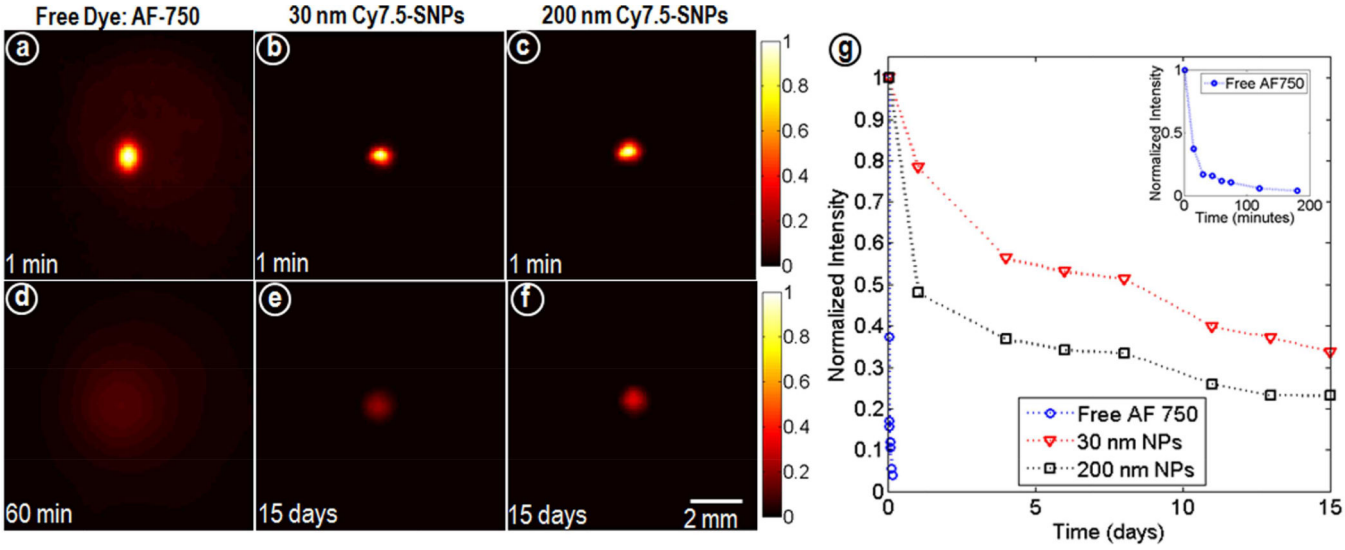

Figure 2.

Fluorescence images of agarose phantoms (n=3) acquired at different time points for (a, d) AF-750*, (b, e) 30nm and (c, f) 200 nm Cy7.5-SNPs and (g) normalized intensity profiles. All acquisition parameters were kept constant and normalized to the maximum at minute 1. *Hydrophilic dye AF-750 was used as free dye as Cy7.5 gets quenched in aqueous media.

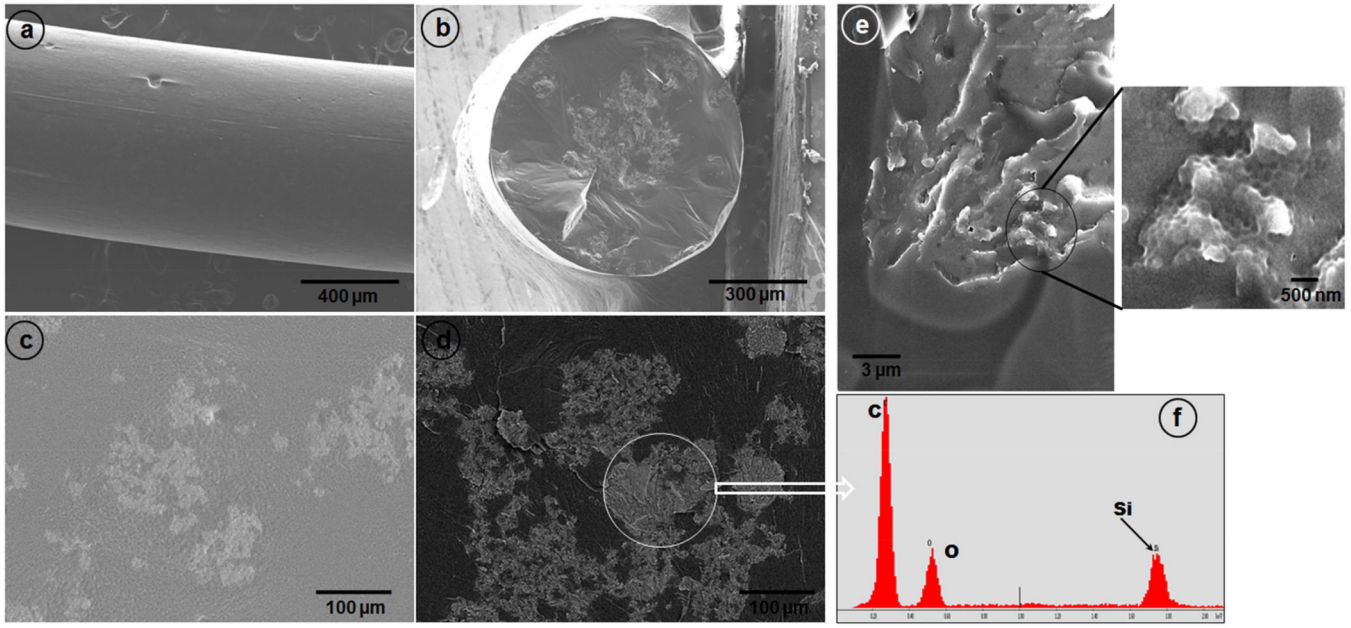

Figure 3.

SEM images of the spacers doped with Cy7.5-SNPs. (a) Lateral surface, (b) transverse view, (c) magnified lateral view, (d) back-scattered electron image of the lateral section, (e) spacer freeze fractured using liquid N_2 (magnified area shows SNPs impressions) and (f) EDS spectra shows the presence of Si in the ROI.

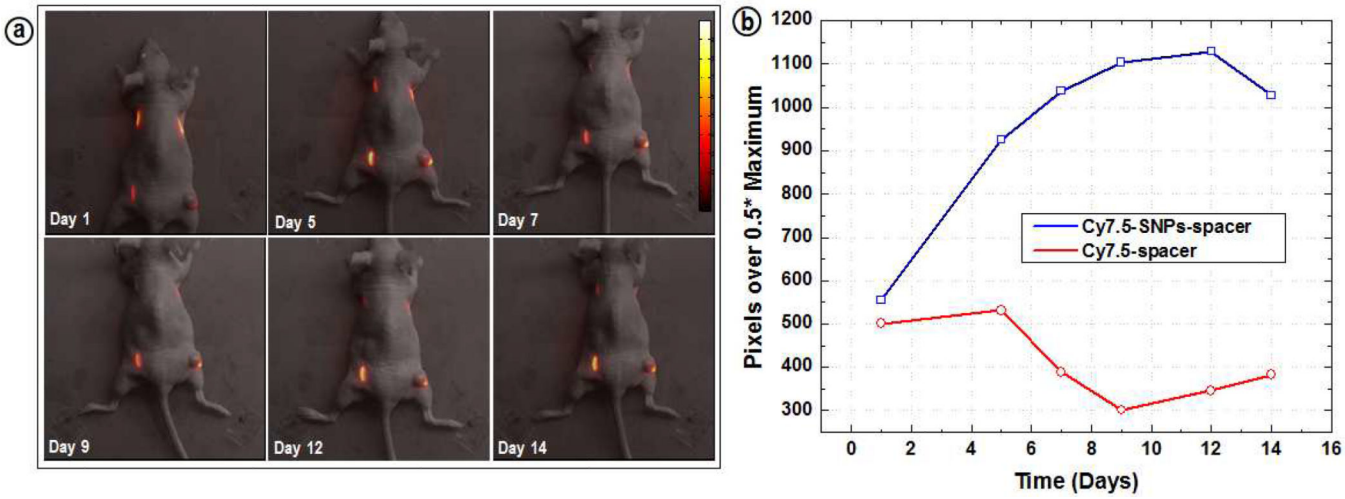

Figure 4.

(a) Live animal *in vivo* optical fluorescence imaging with the mice implanted with Cy7.5-SNPs-/Cy7.5-spacers and (b) quantification of the fluorescence intensity.

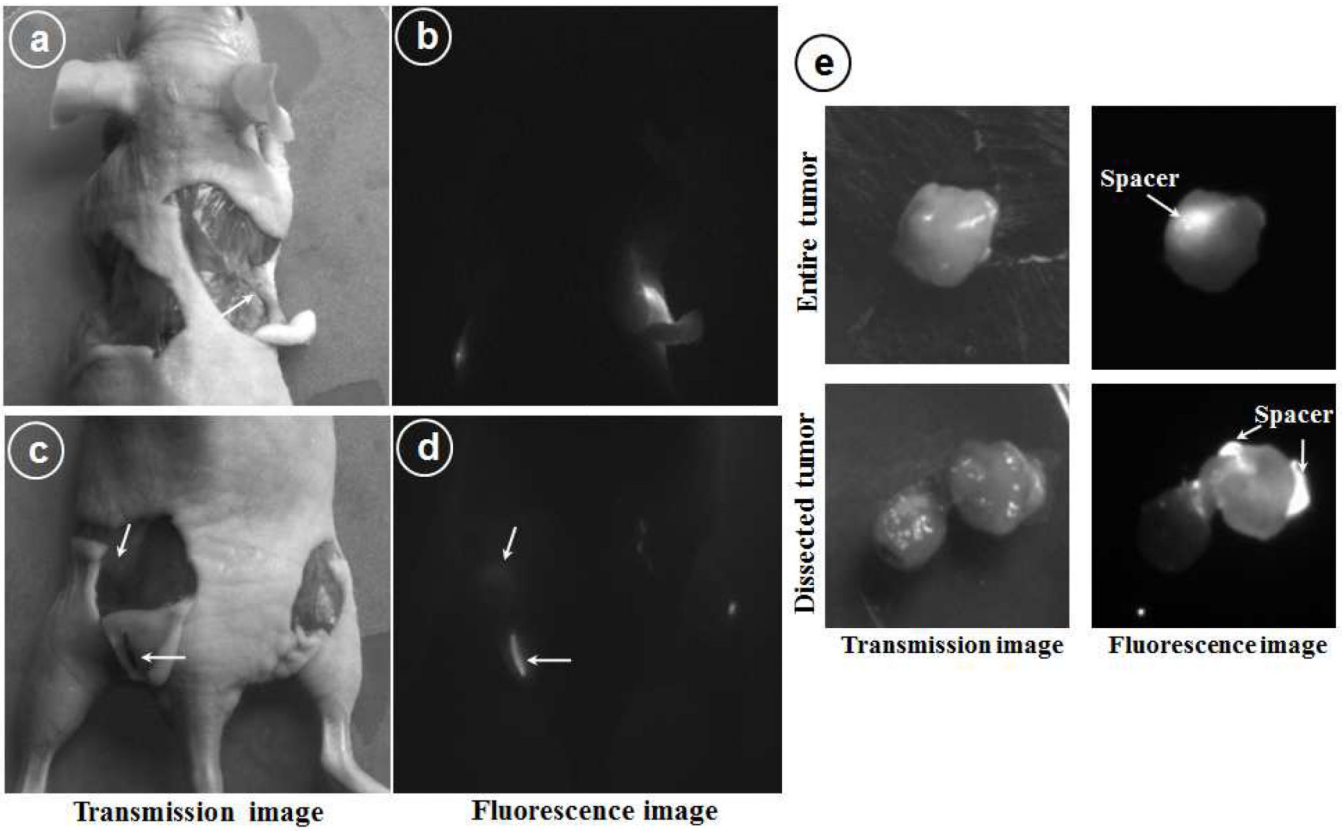

Figure 5.

Optical fluorescence images of the dissected mice 14 days post spacer implantation. (a&b) upper flank to show left Cy7.5-SNPs-spacer and right Cy7.5-spacer, (c&d) hind flank: on left Cy7.5-SNPs-spacer implanted intradermally and right side was implanted intratumorly; (e) Dissected tumor from the mice to locate the implanted spacer inside tumor (upper panel) and lateral section to visualize nanoparticles distribution (lower panel).